

# Monitoring of Non-Linearities in Fatigue Degradation of Metallic Materials Using Techniques beyond Stress and Strain

Christian Boller<sup>1</sup>, ORCID (0000-0003-1142-9390), Peter Starke<sup>2</sup>, ORCID (0000-0002-8033-0602)

<sup>1</sup>Chair of Non-Destructive Testing and Quality Assurance (LZfPQ), Faculty of Natural and Technical Science, Saarland University, Campus Dudweiler, Am Markt Zeile 4, 66125 Saarbrücken, Germany

<sup>2</sup>Materials Science & Materials Testing (WWHK), University of Applied Science Kaiserslautern,

Schoenstraße 11, 67659 Kaiserslautern, Germany

email: c.boller@mx.uni-saarland.de, peter.starke@hs-kl.de

**ABSTRACT:** Traditional fatigue assessment in metals is based on load sequences either measured or assumed, S-N (Wöhler) curves and the application of linearized damage accumulation rules. This requires a large amount of experimental effort to obtain materials data to be used for prognostics of which the result is often unsatisfactory. Furthermore, such assessment is mainly based on stress and strain as the loading parameters applied. However, materials fatigue degradation is a more complex process, far from being linear and not limited to stress and strain only. Material's degradation is an issue. Without knowing a material's prior loading history its degree of degradation can neither be assessed nor monitored on this basis. However, monitoring a material's degree of degradation is a prerequisite to preserve a structure's health over its Residual Useful Life (RUL). Available Non-Destructive Testing (NDT) techniques can be of a significant help. This paper shows how a metallic material's non-linear fatigue behaviour can be visualized in a 3D plot characterizing the loading applied as an input parameter, the NDT parameter recorded as a material response and the relative fatigue life, hence the degree of degradation, as a resulting parameter respectively. It is shown how this resulting 3D viewing plane can be used to determine a material's degree of fatigue degradation at virtually any stage of its operational life and it is demonstrated how this information can be used for a monitoring system in the sense of Structural Health Monitoring (SHM) to further track a structure's RUL in a much more precise way than traditionally done so far.

**KEY WORDS:** Monitoring, non-linear fatigue degradation, Residual Useful Life, metallic materials

## 1 INTRODUCTION

Degradation of materials due to fatigue is a concern scientifically elaborated on since around 150 years. Its traditional assessment is based on load sequences either measured or assumed, S-N (Wöhler) curves and the application of linearized damage accumulation rules. The approaches being applied to experimentally determine a material's fatigue degradation and to get this analytically and/or numerically evaluated has been described in a variety of textbooks (i.e. [1-3]). Although the principles described in those textbooks might be applicable to a variety of materials, these principles have been mainly developed and used so far best with metallic materials. The effort to get the respective materials characterized and data generated is relatively high. To sufficiently cover such materials' fatigue data a set of around 25 fatigue experiments needs to be performed at different loading levels, a significant effort in terms of time and cost. An attempt to optimize this effort has been achieved by collecting and evaluating materials' data for cyclic loading nearly 40 years ago [4,5]. This data has been based on stress and strain as the loading parameters, being the most relevantly used in engineering design today. A major application of this data is within the context of local strain approaches, where the fatigue life of a service loaded notched component is determined with the help of a notch-strain-relationship as proposed by Neuber and others [1-3]. Materials' fatigue data determined on unnotched specimens are therefore the basis to perform a fatigue life evaluation of notched components under service loading. This article will therefore focus on the material's fatigue response and how this could be monitored with

advanced sensing beyond the traditional parameters of stress and strain.

To further enhance the process of materials fatigue data generation in terms of time and cost Short Time Evaluation Procedures (STEP) have been developed, along which the material's stress-strain and S-N behaviour can be determined down to a single fatigue experiment only [6-8]. The logic of those STEP approaches in its earlier form and being applied here is shown in Figure 1. This is based on three fatigue experiments, where two are traditional Constant Amplitude tests (CAT) and one is a Load or a Strain Increase Test (LIT or SIT) respectively, all tests performed on unnotched specimens. A LIT or SIT is a fatigue test, where the specimen is loaded at a constant stress (LIT) or strain (SIT) amplitude for a defined number of time or loading cycles, starting at a small stress/strain amplitude within the material's full elastic range behaviour and then increasing the stress or strain stepwise while keeping the duration of each step in terms of either time or number of cycles constant.

What is determined from the LIT or SIT is a relationship between the load applied (i.e. stress or total strain) versus a respective material response. In traditional terms, this material response is often plastic strain, being one of the mechanisms associated with fatigue in metals. Morrow [9] was possibly one of the first who determined such a relationship in terms of the strain hardening exponent  $n'$  of a metallic material's stress versus plastic strain relationship proposed as

$$\varepsilon_{a,p} = \varepsilon_f' \cdot \left( \frac{\sigma_a}{\sigma_f'} \right)^{1/n'} \quad (1)$$

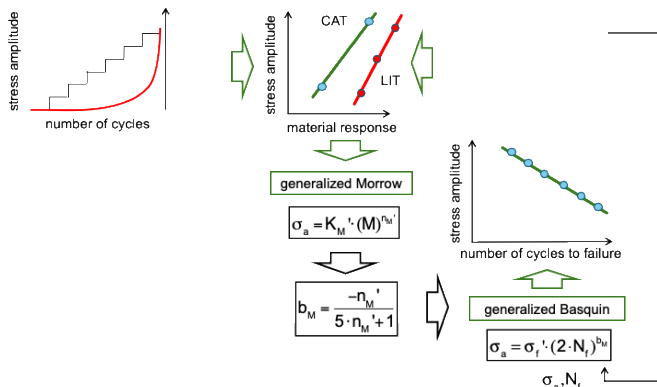


Figure 1 Logic of a STEP approach for the quick determination of an S-N curve

where  $\varepsilon_{a,p}$  represents the plastic strain amplitude,  $\sigma_a$  the applied stress amplitude, and  $\varepsilon_f'$  and  $\sigma_f'$  are constants referred to as the cyclic ductility and strength respectively similar to the true fracture ductility and strength under tensile monotonic loading. Morrow also used the two latter constants to describe a material's strain-life curve in the form of

$$\varepsilon_{a,t} = \frac{\sigma_f'}{E} (2N_f)^b + \varepsilon_f' (2N_f)^c \quad (2)$$

where  $\varepsilon_{a,t}$  is the total strain amplitude as an addition of elastic and plastic strain,  $E$  Young's modulus,  $N_f$  the number of cycles to failure and  $b$  and  $c$  the slopes of the life curves for elastic and plastic strain when being plotted in a double logarithmic scale respectively. What Morrow further did was to establish a relationship between the slopes  $b$  and  $c$  on the one side and the strain hardening exponent  $n'$  on the other resulting in

$$c = \frac{-1}{1+5n'} \text{ and } b = \frac{-n'}{1+5n'} \quad (3)$$

allowing a fatigue life (S-N) curve to be determined from a material's strain hardening response in the end. This relationship has also been used in the STEP procedures mentioned above in a slightly modified way, differentiating between the elastic and the plastic material behaviour.

Sensing and hence monitoring of a material's behaviour today can go far beyond monitoring stress and strain only. Non-Destructive Testing (NDT) has opened a large gamut of options considered in the past with respect to fatigue life evaluation and hence, residual life assessment of engineering structures, of which the potential has only been explored to a limited extent in the past. However, where this has been considered is in the context of STEP and here with respect to what has been considered as the 'material response' shown in the diagram in Figure 1. Examples presented in [6-8] and in various other publications do include techniques such as infrared thermography, electrical resistance and eddy current measurement. In this paper the case of thermography is presented and how this can be used for characterizing a metallic material's fatigue degradation behaviour. The information obtained is intended to be used for monitoring existing engineering structures, for which the degree of fatigue degradation due to a missing crack observation is unknown but where through monitoring an improved Residual Useful Life

(RUL) assessment of the metallic engineering structures is in need.

## 2 THERMOGRAPHY INSPECTION OPTIONS

Thermography is an electromagnetic NDT technique, along which a specimen is viewed with an infrared (IR) camera. The camera used here has been a thermoIMAGER TIM 450 from Micro-Epsilon, which is based on a bolometer-based pixelized image of 382 x 288 pixels with a sensitivity of  $\geq 40$  mK each. A view of such a set-up as well as a resulting image is seen in Figure 2. Temperatures are continuously recorded on the unnotched specimens in a fatigue test in the three zones indicated as  $T_1$  to  $T_3$ . From the data recorded a temperature difference  $\Delta T$  is then determined in accordance with the following equation:

$$\Delta T = T_3 - \frac{T_1 + T_2}{2} \quad (4)$$

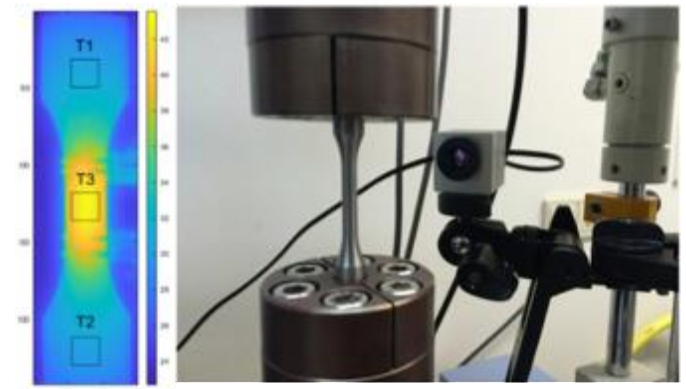


Figure 2 Thermographic monitoring on unnotched specimen under fatigue loading: View of the specimen through thermographic camera including measurement points (left), experimental set-up (right)

## 3 THERMOGRAPHY BASED FATIGUE DATA

Metallic materials' data for cyclic loading are traditionally determined under either stress or strain control and are represented in terms of stress-strain relationships and the number of loading cycles up to failure (S-N curves). This data may be used for fatigue life evaluation of engineering structures under cyclic service loading, where mainly linearized damage accumulation rules such as proposed by Palmgren [10] and Miner [11] are applied. Results obtained often show a certain randomness (scatter) and the reasons for this can be sought in non-linearities a material provides. A question therefore arises what additional material response information could be retrieved in case of data being recorded with an NDT technique. In the case shown here, unnotched specimens made of the unalloyed steel C45E (1.1191 or SAE 1045) have been fatigue loaded as CATs at different stress and strain amplitudes and a LIT and SIT respectively and this under stress as well as strain control and at partially different loading frequencies. The full test set-up is shown in Figure 3.

Three CATs were performed under stress control at amplitudes of 320, 340 and 360 MPa and resulting fatigue lives of 109 408, 14 957 and 16 294 cycles respectively were obtained. The reason why the fatigue life of the test run at  $\sigma_a =$

360 MPa is higher than the fatigue life for the test run at  $\sigma_a = 340$  MPa is due to scatter in the fatigue life and the proximity of the stress amplitudes. The  $\varepsilon_{a,t} - N$  curve shown in Figure 4 that the experimental results show a typical fatigue behaviour. In addition, a LIT was performed starting at a stress amplitude of 100 MPa and being increased by 20 MPa always after 9 000 cycles until it reached a stress amplitude of 380 MPa. All of those tests were operated at a loading frequency of 5 Hz. These experiments were part of a master thesis performed [12].

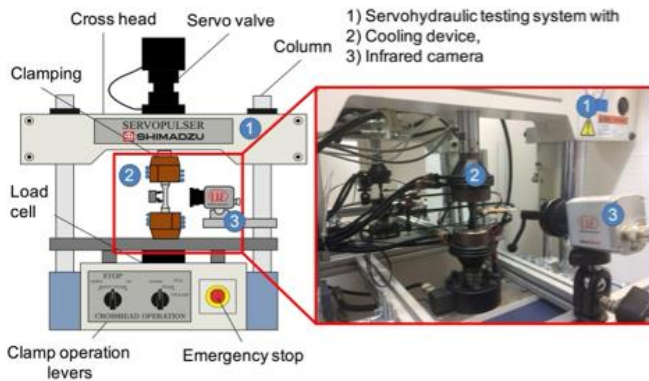


Figure 3 Test setup for recording thermographic data along fatigue experiments on unnotched specimens: 1) test frame, 2) clamped specimen, 3) IR camera

In addition, two CATs and a SIT were performed on the same material but now under a sinusoidal function in strain control mode and considering a constant average strain rate of 1.0 %/sec or a maximum strain rate of 1.57 %/sec respectively. The strain amplitudes for the CATs were  $\varepsilon_{a,t} = 1.0$  % and  $\varepsilon_{a,t} = 0.3$  % respectively while the SIT started at a strain amplitude of  $\varepsilon_{a,t} = 0.1$  % and was increased by 0.02 % after every step of 2 000 cycles until it fully failed at a strain amplitude of  $\varepsilon_{a,t} = 0.42$  %. The fatigue lives of the two CATs up to full fracture was 600 and 14 600 loading cycles respectively.

Based on this data STEP as described before was applied to determine the S-N data. Figure 4 shows the results in terms of the stress vs. plastic strain relationship as well as the strain-life curve. The exponent  $n'$  from Eq. 1 turned out to be -0.122 which allowed the exponents for the  $\varepsilon_{a,t} - N$  curve to be determined according to Eq.s 3. Coefficients  $\sigma_f'$  and  $\varepsilon_f'$  were determined from the results of the two strain-controlled CATs through averaging. The resulting  $\varepsilon_{a,t} - N$  curve very well matches the remaining experimental results used for validation.

A summary of the thermographic recordings is provided in Figure 5. It shows the relationship of the temperature difference  $\Delta T$  due to fatigue loading versus a normalized fatigue life. This normalization has been determined on the fatigue life of each of the experiments shown here. This can also be considered as the degree of degradation, specifically for the CATs, where the Palmgren-Miner rule applies per se. Why this has also been done for the LIT and the SIT is for reasons of comparison with some further explanation later. What can be seen at this stage is that the stress levels match fairly well between the stress-controlled CATs and the LIT. When looking at the strain-controlled tests the SIT generates higher temperature differences when compared with a CAT at the same strain level.

What is also to be observed from Figure 5 is, that the temperature difference  $\Delta T$  seems higher for the stress-controlled experiments than it is for the strain-controlled tests. However, it has to be kept in mind, that the loading frequency for the stress-controlled tests was always 5 Hz while the strain-controlled tests were done at a constant maximum strain rate of 1.57 %/sec and the loading frequency hence varied between 0.25 and 2.5 Hz only. Following these results, it might be worth to explore, which loading parameters do have an influence on the temperature difference  $\Delta T$ . The reason why the temperature drops after each loading step in the SIT is due to the fact that loading is briefly interrupted and the new loading step is started with a gradual increase of the load applied. This effect has not been further considered in the evaluation.

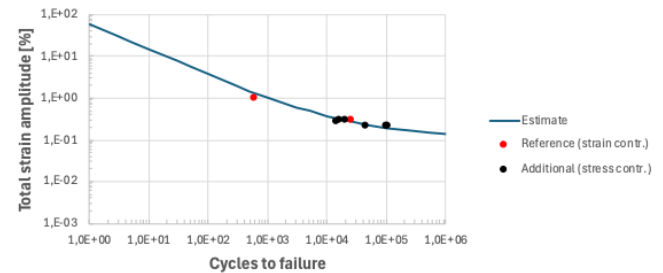
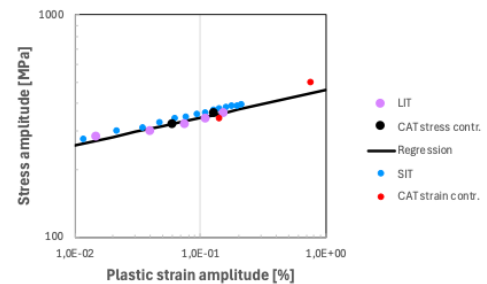


Figure 4 Results of fatigue tests performed presented as a stress vs. plastic strain relationship (top) and  $\varepsilon_{a,t} - N$  curve (bottom) both in a double logarithmic scale

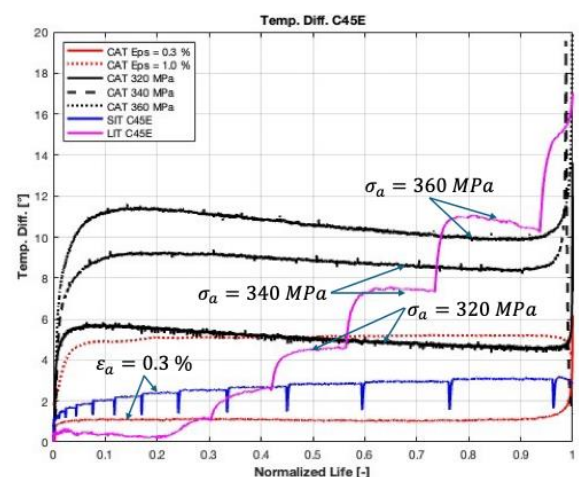


Figure 5 Development of temperature difference in three CATs and one LIT over normalized life of the CATs obtained under stress-controlled fatigue loading



All the experiments presented here were analysed with respect to stress amplitude and maximum strain rate vs.  $\Delta T$  and the result obtained is shown in Figure 6. It can be seen that as long as no plastic deformation occurs  $\Delta T$  remains marginal. Hence, any significant influence on  $\Delta T$  is governed by loading parameters in the plastic deformation region. The relationship between plastic strain and  $\Delta T$  can be linearized but this depends on the loading conditions (i.e. stress- or strain-controlled) and only when those are similar, a single function can be drawn, as to be seen from the fatigue test data shown in Figure 7.

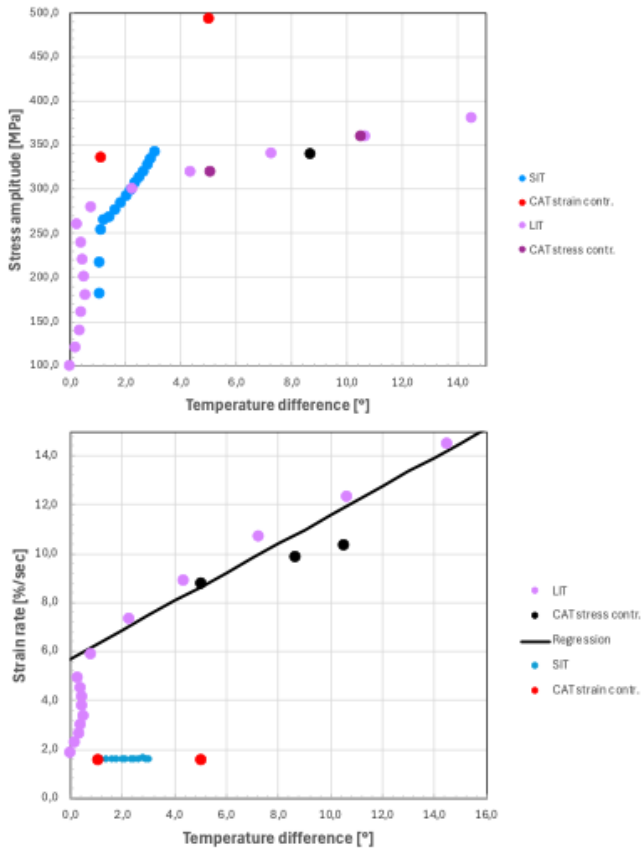


Figure 6 Stress vs.  $\Delta T$  (top) and strain rate vs.  $\Delta T$  (bottom) for all CATs, LIT and SIT performed

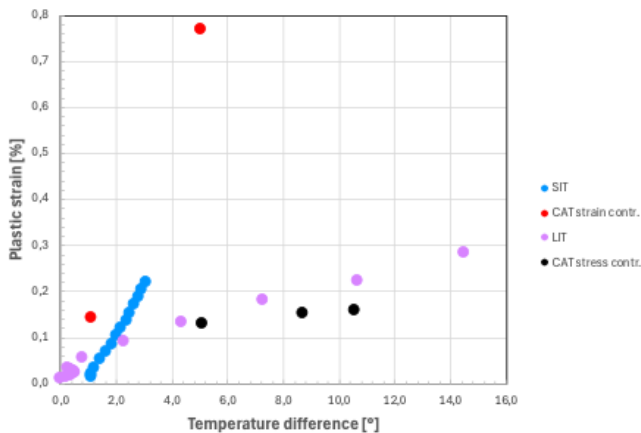


Figure 7 Plastic strain vs.  $\Delta T$  for all CATs, LIT and SIT performed

Energy is another parameter worth to be considered in that regard where the Smith-Watson-Topper (SWT) parameter [13] also known as the Neuber-parameter is widely used in the field of fatigue life evaluation of notched components and which is defined as:

$$P_{SWT} = \sqrt{\sigma \cdot \varepsilon_t \cdot E} \quad (5)$$

where  $\sigma$  represents the stress,  $\varepsilon_t$  the total strain and  $E$  Young's modulus respectively. If the fatigue results of this parameter are plotted versus  $\Delta T$  a result as shown in Figure 8 is obtained. The figure shows a lot of similarities to Figure 6 (top) and Figure 7 which is not much of a surprise. However, also in the case of energy no consistency in the thermographic material response can be observed. What can already be concluded here is that stress-controlled loading conditions can be better monitored with thermography than strain-controlled conditions can.

A question that might arise is, what would happen if a fatigue test could be performed where the energy applied could be permanently kept constant (controlled). First of all, this is a fairly complex fatigue test, which can be performed and has been specified as Neuber-controlled but which requires stress and strain to be controlled at the same time [14]. This could lead to some consistency between loading and the material's thermographic response and hence way of further validation. However, when looking plastic deformation in the roots of notched components, those plastic zones are mainly strain-controlled due to the elastic field around this plastic zone. Furthermore, energy conditions change along the life cycle of a material due to hardening and softening conditions resulting from the loading history.

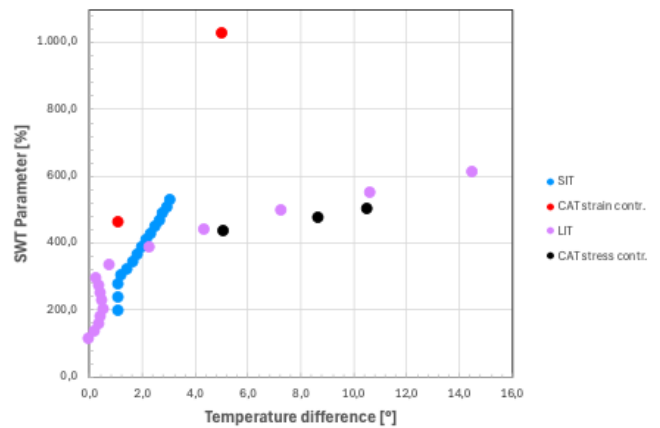


Figure 8 Energy expressed in terms of the Smith-Watson-Topper parameter vs.  $\Delta T$  for all CATs, LIT and SIT performed

As a consequence of all having been presented so far, the plastic strain rate as well as the stress range above the yield strength looks to be mainly influential on  $\Delta T$ . As such a thermography-related loading parameter  $P_T$  is defined as to the following:

$$P_T = \varepsilon_{a,p} \cdot \omega \cdot (\sigma_a - \sigma_y) \quad (6)$$

where  $\varepsilon_{a,p}$  is the plastic strain amplitude,  $\omega$  the circular frequency of the loading,  $\sigma_a$  the stress amplitude and  $\sigma_y$  the yield stress respectively, the latter determined as 255 MPa from the upper diagram in Figure 6. Plotting all the experimental results as  $P$  vs.  $\Delta T$  leads to the diagram shown as Figure 9, which allows a concise relationship to be determined in linear or close to linear format.

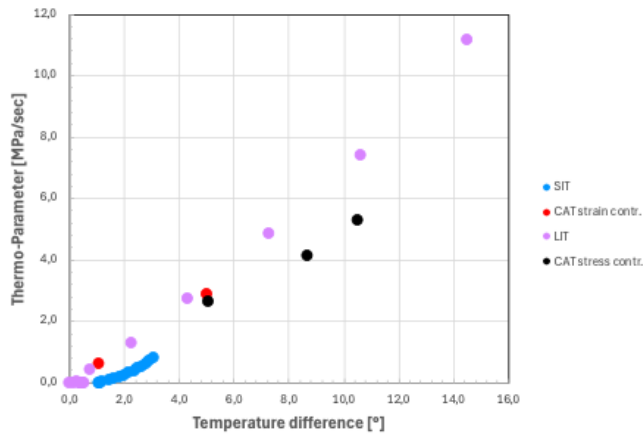


Figure 9 Loading parameter  $P_T$  vs. temperature difference  $\Delta T$  for all CATs, LIT and SIT performed

Since the temperature difference  $\Delta T$  recorded is a material response, its possible non-linear behaviour raises certainly the question what of a material's non-linear behaviour it represents and if the consideration of such non-linearity might better cover a metallic material's non-linear fatigue degradation than this has been possible to be covered in the past. To get this shown a 3D plot has been generated representing temperature difference  $\Delta T$  recorded (z-axis) versus the enforcement applied represented by the parameter  $P_T$  (y-axis) and the fatigue life for the CATs in a normalized form (x-axis). What the latter axis therefore represents is nothing else than the degree of degradation.

Such a result is shown in Figure 10 for the five CATs (stress and strain controlled) as well as the LIT and the SIT. In the case of the CATs the temperature increases immediately at the beginning since in all cases yield is passed and plastic deformation has occurred. Once plastified, the temperature increase looks fairly constant over the lifetime of the specimens until final fracture occurs. The strain-controlled tests show less of a temperature increase when compared to the stress-controlled tests. Principally they align well with the parameter  $P_T$  defined in Eq. 6. Furthermore, these test results can serve as a basis to generate a plane as shown in Figure 11 characterizing the material's fatigue as well as monitoring behaviour, which is discussed later.

When looking at the results from the LIT and the SIT a fairly different behaviour is observed. While the SIT due to its constant strain rate shows a relatively continuous behaviour with slight temperature increases observed due to the slight increases in strain amplitudes and loading in terms of the parameter  $P_T$ , the LIT and the way it has been performed shows a fundamentally different behaviour with significant changes in temperature due to the significant changes from loading step to loading step. However, the results of both tests fairly well align

in the plane described by the CAT results keeping potential scatter in materials' data in mind. It might therefore be worth considering such planes as a material's characteristic along which the results of any loading sequence might move. Further proof of those assumptions with more complex loading sequences might be advisable for the future.

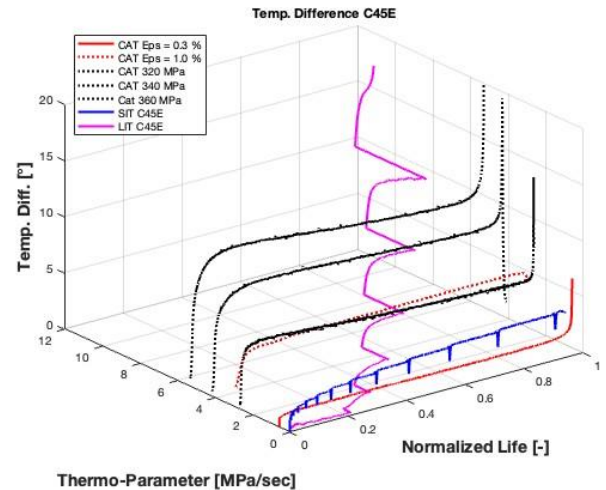


Figure 10 Development of temperature difference  $\Delta T$  in dependence of power rate applied and normalized fatigue life of CATs and comparison with the same relationship obtained from LIT and SIT

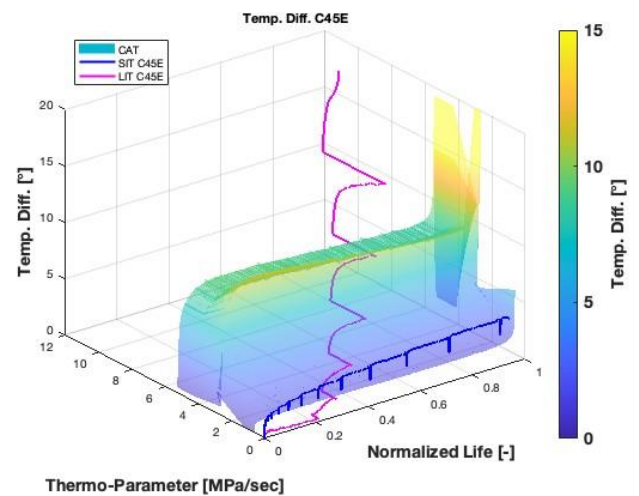


Figure 11 Topography of temperature difference  $\Delta T$  vs. power rate  $P$  and normalized life relationship for CATs and compared with similar results obtained from LIT and SIT

Since the stress, strain and loading frequency are the controlled and hence known input values related to the material's loading and  $\Delta T$  the material response monitored, the remaining unknown value is just the normalized life or in other words, the degree of degradation when talking in terms of the Palmgren-Miner rule, at least related to CATs. To get this degree of degradation obtained it has been assumed that the Palmgren-Miner rule applies for CATs and that as such the amount of degradation can therefore be calculated for each of the loading blocks or even loading cycles of the LIT and the

SIT. This leads to a description of the degradation development being very much different, as can be seen from Figure 12. The degradation process for the SIT and specifically for the LIT looks very much slower and the estimated fatigue life looks to be expired before plastic deformation even starts off in the case of the LIT. This contradicting result might be another proof of the lack of precision when applying Palmgren-Miner's rule. A conclusion is therefore, that monitoring the temperature emitted from a loaded structure might be the better information to determine a structure's degree of degradation than performing a Palmgren-Miner evaluation in traditional terms.

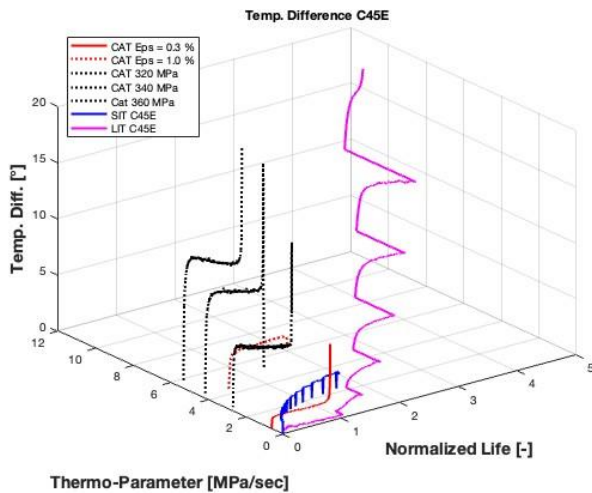


Figure 12 Development of temperature difference  $\Delta T$  over the CATs' normalized fatigue life and determining the respective fatigue life of the LIT and SIT through application of the Palmgren-Miner rule

#### 4 TEMPERATURE DIFFERENCE FOR MONITORING

SHM is based on using a material's response information to assess a structure's degree of degradation. Hence, the material's information provided through a diagram as shown in Figure 11 might therefore be a valuable tool to assess the structure as well as the monitoring principle being considered. A temperature difference resulting from a load applied on a structure and monitored through SHM could be principally used to be referenced to a diagram as shown in Figure 11. Assuming the respective value monitored on the structure could be determined as a single value on such a reference diagram, the degree of the structure's degradation could be easily determined. However, if such a value turns up more than once on the plane of the reference diagram, a conflict arises, which needs to be solved through more information to be retrieved. A help might be to mark the respective value positions on the diagram, which might even be described as isobars. Based on those isobars the appropriate solution needs to be found, which might be possible either through a variation (differentiation) in the direction of the power rate  $P_T$  and/or the normalized fatigue life.

As for the specific case of using thermography as the monitoring principle and the material as shown here, the situation in getting useful information from such a differentiation becomes tricky. The plane described in Figure

11 is mainly flat in the direction of the normalized life of the CATs. It looks like the material characterized becomes immediately plastified and this condition stays until fracture occurs towards the end of the tests. Thermography as a monitoring technique therefore clearly demonstrates, that it can identify plastic deformation but obviously not its contribution to fatigue degradation in the end. Also, the plane's inclination in the direction of the power rate  $P_T$  is fairly constant. Hence, the variation of loading parameters along the monitoring process might not provide the information to sufficiently identify the degree of material degradation.

However, the principle of a 3D plot as shown here in Figures 10 and 11 might be a useful instrument to collect and visualize data monitored as a combination of load, loading frequency and temperature on either a real structure or an unnotched specimen - of course of the same type of material. A summarized dataset shows in such a 3D plot if the data do represent a plane and which uncertainties might exist, to get this plane described or in other words how scattered the data recorded might be. Based on such scattered data allowance criteria might then be defined. Maybe that a longer-term monitoring on a structure to be assessed generating a larger database and combined with some advanced statistical evaluation might help to identify an appropriate location on the plane of the 3D plot and hence determine the degree of the structure's degradation. However, this requires further evaluation, which has not been performed so far.

In the context of the thermographic data presented here another aspect might be worth to be discussed. Thermography looks to be a method to allow plastic deformation in metals to be monitored well. This could make it interesting to identify plastic deformation in stress concentrated areas such as in notches. However, one needs to keep in mind, that fatigue loaded plastic zones in stress concentrated areas of notches are loaded in a strain-controlled mode. The reason for this is due to the elastic deformation occurring around the plastic zone. Hence, if those plastic zones might be monitored with thermography one should not be astonished if the signal might be weak, as concluded from results shown in Figures 5 and 6.

#### 5 CONCLUSIONS

The results presented here are far from claiming to be holistic. They are rather an additional extraction of data having been recorded along tests to establish S-N curves in accordance with the STEP approach. However, what proves to be interesting is to find out if an NDT method considered might be useful in terms of SHM and this in view of monitoring a material's and even a structure's degree of degradation with respect to fatigue. Compared to state-of-the-art approaches where monitoring is just possible in terms of detecting loads, strains and cracks, monitoring based on thermography at least allows plastic deformation to be identified additionally, a precursor to fatigue cracking.

While it has been shown here that loading, plastic deformation and of course also cracking can be measured through a temperature difference  $\Delta T$ , further parameters inherent in thermography signals might be worth to be explored. This may be achieved through higher sampling rates of the thermographic data and might allow the signal recorded to be better evaluated in terms of time domain information



including phase. Further extensions could be made in view of active thermography.

Generalizing the approach made here to virtually any monitoring and hence NDT technology to be considered for SHM could be a means to assess the NDT technology's potential with respect to SHM. A further step could be to differentiate the 3D plane obtained and shown in Figure 11 either in terms of the power parameter  $P_T$  or the normalized fatigue life. This would lead to a new 3D plot that would either characterize the material's sensitivity with respect to the loading or the fatigue life. In case of the fatigue life such differentiation might be a more sensitive parameter in identifying the degree of degradation and this also with respect to monitoring. However, this requires the 3D plane not to be as flat as in the case shown here, since a differentiation of this plane leading to a 3D gradient plot otherwise just scatters around zero. Such flatness of the 3D plane and scattering around zero in the 3D gradient plot might therefore also be an indication that the monitoring technique is possibly not suitable for monitoring a material's fatigue degradation in the pre-cracked stage.

The topography of the 3D plot shown in Figure 11 is also an indication of the non-linearity the monitoring parameter exhibits and this with respect to a potential non-linearity in the material. Hence, if the 3D plot is relatively 'flat' and constant in its height, this could mean that linearization of fatigue degradation for the respective material and hence the traditional Palmgren-Miner rule would be better applicable when compared to materials where such a topography of the 3D plane might be more uneven. However, in the case here it at least shows for the LIT and the SIT that irrespective of the smooth surface the predictions are not very consistent and the material response recorded might not work very well in combination with the Palmgren-Miner rule (c.f. Figure 12). Further corrections might therefore have to be done to get this improved. Or formulated inversely as a question: Would a 'wavy' or possibly more 'spiky' 3D plane characterize a monitoring technology as a more relevant technology for monitoring fatigue degradation? Furthermore, could a 'spiky' 3D plane possibly be used to enhance a component's fatigue life under service loading evaluation since it better covers the material's non-linearities in fatigue degradation than the Palmgren-Miner rule is able to do? Answers to these questions might be obtained through a further random load fatigue assessment.

Should any if not all of those questions be answered positively, then the diagrams as shown in Figures 10 and 11 might become future displays of materials' data for cyclic loading, representing a clear extension when compared to the traditional stress-strain and S-N curves provided in handbooks such as [4,5] in the past. Interesting additional questions in that regard are also if the 'life path' of a randomly loaded material follows the topography spanned by the CAT results. In case of a match every data recorded could be virtually added to the database, allowing the material's information to continuously grow.

What has been shown here with the SIT results is, that the temperature difference  $\Delta T$  mainly stays or marginally increases on an isobar during each loading step when the strain is increased from one strain level to another. However, what

happens with this path when the strain levels are decreased is still an open question to be answered.

The large amount of data being recorded might also become an interesting source for statistical evaluations. Monitoring an engineering structure under service loading with a thermographic camera combined with other loading parameters might provide an interesting data sample for a further statistical evaluation of which the statistical patterns might be correlated with patterns to be found in the material's general reference database.

The approach presented here intends to show how far thermography might be applicable in the context of SHM. At present the monitoring principle has been proven for a laboratory environment only. The major sensing device is the IR camera which has to stay as an external device. An interesting next step to explore would be to perform the same type of fatigue experiment but with larger, more complex, notched components and to see how well the fatigue behaviour in the notches could be monitored. A constraint might be the strain-controlled mode and the resolution of the IR camera system as well as the component's shape for which corrections might have to be made regarding the signals to be processed. Another aspect to be explored is the influence of the component's surface preparation. It is very likely that a quantitative validation of a component as is might not lead to satisfying results and that coatings might have to be removed and/or treated such that comparable conditions are achieved. This is an important step that has to be proven before considering any in field monitoring in terms of general applications. Potential first applications could be seen for fatigue loaded components being visually easily accessible and highly loaded, preferably considering a load spectrum to be 'sharp', hence, with a large number of high loads. Again, a potential application could be in the field of testing of fatigue loaded components and assessment of their degradation processes in a laboratory environment. Another field would be rotating machinery where the rotating rod is just fixed with bearings, but all other parts are visually easily accessible. However, a new challenge might arise between the rotating frequency of the machinery versus the frame rate of the IR camera.

A solution to all those challenges could be temperature sensors, that could be directly adapted onto the structure to be monitored but this is far from being realized at present. However, the approach presented here is not limited thermographic monitoring only. Eddy current or other electromagnetic sensors being commercially available are sensors that can already be attached in situ and where the 3D plot can be generated as the source of reference. In that case, civil infrastructure could be an interesting application field.

All what has been described here is related to passive thermography only. What active thermography would provide is an additional chapter being beyond the scope of this article.

A further challenge comes if those monitoring approaches might be applied in the field where a thermographic camera records a structure in service under general environmental conditions. In that case all environmental influences will have to be compensated such that only the true difference due to degradation becomes apparent in the thermographic analysis.

As such passive thermography in SHM of mechanically loaded structures is still limited to fundamental explorations that may provide the appropriate parameters to be considered for a more generalized application in structural life cycle management.

## REFERENCES

- [1] E. Haibach: Betriebsfestigkeit, Springer Berlin & Heidelberg, (2006) doi.org/10.1007/3-540-29364-7 (in German)
- [2] D. Radaj, M. Vormwald: Advanced Methods of Fatigue Assessment; Springer Berlin & Heidelberg (2013) doi.org/10.1007/978-3-642-30740-9
- [3] J. Schijve: Fatigue of Structures and Materials; Springer (2009)
- [4] C. Boller and T. Seeger: Materials Data for Cyclic Loading, Vol.s A to E. Elsevier Science Publ. (1987)
- [5] A. Bäuml jr. and T. Seeger: Materials Data for Cyclic Loading (Supplement); Elsevier Science Publ. (1990)
- [6] P. Starke, F. Walter and D. Eifler: PhyBaL – A new method for lifetime prediction based on strain, temperature and electrical measurements; Int. J. of Fatigue 28 (9), (2006), 1028-1036
- [7] P. Starke: Lebensdauerberechnung bei ein- und mehrstufig beanspruchten Proben aus vergütetem 42CrMo4; Dr.-Ing. thesis, TU Kaiserslautern (2007) (in German)
- [8] P. Starke, H. Wu, C. Boller: Advanced evaluation of fatigue phenomena using non-destructive testing methods, Materials Science Forum 879 (2016) 1841-1846
- [9] J.D. Morrow: Cyclic Plastic Strain Energy and Fatigue of Metals; ASTM STP 378, (1965) 45-87
- [10] A. Palmgren: Die Lebensdauer von Kugellagern, Z. VDI 68 (14), (1924), 339-341 (in German)
- [11] M.A. Miner: Cumulative damage in fatigue, J. of Appl. Mech. 12, (1945), A159-A164
- [12] B.D. Yesa: Analysis of the reproducibility of thermographic data under different external condition; Master thesis at Dresden Internat. Univ. (DIU) and LZfPQ Saarland Univ. (2022)
- [13] K.N. Smith, P. Watson, T.H. Topper: A Stress-Strain Function for the Fatigue of Metals, J. of Materials, IMLSA, Vol. 5, No. 4, (1970) 767-778
- [14] P. Heuler: Crack Initiation Life Prediction for Variable Amplitude Loading Based on Local Strain Approach; Doctoral thesis at Technische Hochschule Darmstadt (1983) (in German)